

# Chaos in Hamiltonian nonlinear lattices

**Haris Skokos**

**Department of Mathematics and Applied Mathematics  
University of Cape Town  
Cape Town, South Africa**

**E-mail: [haris.skokos@uct.ac.za](mailto:haris.skokos@uct.ac.za)**

**URL: [http://math\\_research.uct.ac.za/~hskokos/](http://math_research.uct.ac.za/~hskokos/)**

**29th School – Conference On Dynamical Systems And Complexity  
18 July 2023, Athens, Greece**

# University of Cape Town (UCT)



# University of Cape Town (UCT)



# Cape Town



# Outline

- **The one-dimensional quartic disordered Klein-Gordon (1D DKG) model: Different dynamical regimes**
- **Maximum Lyapunov Exponent (MLE): strength of chaos**
- **Deviation Vector Distributions (DVDs): mechanisms of chaotic spreading**
- **Frequency Map Analysis (FMA): characteristics of spatiotemporal evolution of chaos**
- **Generalized Alignment Index (GALI): localized vs. spreading chaos**
- **Summary**

# The one-dimensional disordered Klein Gordon model (1D DKG)

$$H = \sum_{l=1}^N \frac{p_l^2}{2} + \frac{\tilde{\varepsilon}_l}{2} u_l^2 + \frac{1}{4} u_l^4 + \frac{1}{2W} (u_{l+1} - u_l)^2$$

with **fixed boundary conditions**  $u_0=p_0=u_{N+1}=p_{N+1}=0$ . Typically  $N=1000$ .

Parameters:  $W$  and the **total energy**  $H$ .  $\tilde{\varepsilon}_l$  chosen uniformly from  $\left[\frac{1}{2}, \frac{3}{2}\right]$ .

Linear case (neglecting the term  $u_l^4/4$ )

**Ansatz:**  $u_l = A_l \exp(i\omega t)$ . **Normal modes (NMs)  $A_{\nu,l}$  - Eigenvalue problem:**

$$\lambda A_l = \varepsilon_l A_l - (A_{l+1} + A_{l-1}) \text{ with } \lambda = W\omega^2 - W - 2, \quad \varepsilon_l = W(\tilde{\varepsilon}_l - 1)$$

**Anderson localization** [Anderson, Phys. Rev. (1958)]. Experiments on BEC [Billy et al., Nature (2008)]

**What happens in the presence of nonlinearity?**

**Will nonlinearity destroy localization?**

# Characteristics of energy distributions

We consider normalized **energy distributions**  $\xi_l = \frac{H_l}{\sum_m H_m}$

with  $H_l = \frac{p_l^2}{2} + \frac{\tilde{\epsilon}_l}{2} u_l^2 + \frac{1}{4} u_l^4 + \frac{1}{4W} (u_{l+1} - u_l)^2$

**Second moment:**  $m_2 = \sum_{l=1}^N (l - \bar{l})^2 \xi_l$  with  $\bar{l} = \sum_{l=1}^N l \xi_l$

**Participation number:**  $P = \frac{1}{\sum_{l=1}^N \xi_l^2}$

measures the number of stronger excited sites in  $\xi_l$ .

Single site  $P=1$ . Equipartition of energy  $P=N$ .

# Different dynamical regimes

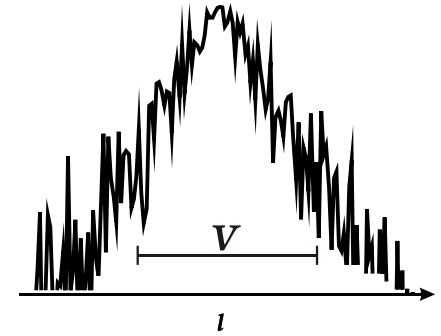
**Three expected evolution regimes** [Flach, Chem. Phys (2010) - S. & Flach, PRE (2010) - Lapyteva et al., EPL (2010) - Bodyfelt et al., PRE (2011)]

**$\Delta$ : width of the frequency spectrum.**  $\Delta = 1 + \frac{4}{W}$  since  $\omega_v^2 \in \left[\frac{1}{2}, \frac{3}{2} + \frac{4}{W}\right]$

**$d$ : average spacing of interacting modes.**  $d \approx \frac{\Delta}{V}$ ,

**$V$ : localization volume of an eigenstate**  $V \sim \frac{1}{\sum_{l=1}^N A_{v,l}^4}$

**$\delta$ : nonlinear frequency shift.**  $\delta_l = \frac{3H_l}{2\tilde{\epsilon}_l} \propto H$



**Weak Chaos Regime:**  $\delta < d$ ,  $m_2 \propto t^{1/3}$  ( $P \propto t^{1/6}$ )

Frequency shift is less than the average spacing of interacting modes. NMs are weakly interacting with each other. [Molina, PRB (1998) – Pikovsky & Shepelyansky, PRL (2008) – Flach et al., PRL (2009)].

**Strong Chaos Regime:**  $d < \delta < \Delta$ ,  $m_2 \propto t^{1/2}$  ( $P \propto t^{1/4}$ )  $\rightarrow m_2 \propto t^{1/3}$

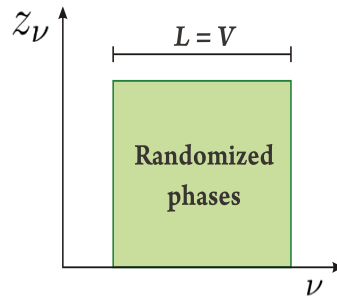
Almost all NMs in the packet are resonantly interacting. Wave packets initially spread faster and eventually enter the weak chaos regime.

**Selftrapping Regime:**  $\delta > \Delta$

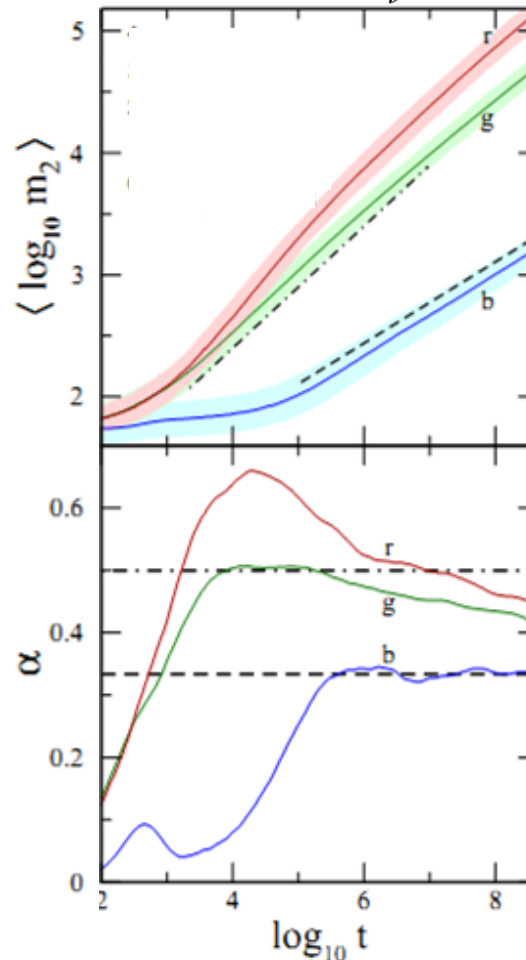
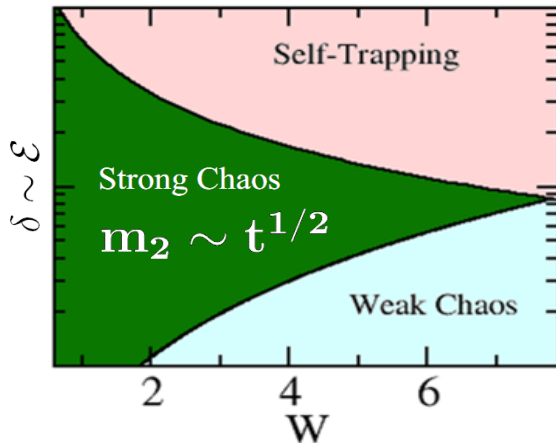
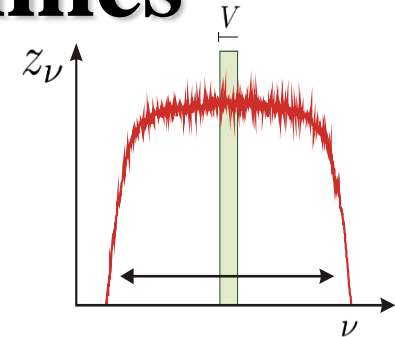
Frequency shift exceeds the spectrum width. Frequencies of excited NMs are tuned out of resonances with the nonexcited ones, leading to selftrapping, while a small part of the wave packet subdiffuses [Kopidakis et al., PRL (2008)].

# Strong and weak chaos regimes

We consider **compact initial wave packets of width  $L$**   
 [Laptyeva et al., EPL (2010)  
 – Bodyfelt et al., PRE (2011)]



Time evolution  $\rightarrow$



$H = 0.01, 0.2, 0.75$

$W = 4$

Average over 1000 realizations!

$$\alpha(\log t) = \frac{d\langle \log m_2 \rangle}{d \log t}$$

# Maximum Lyapunov Exponent (MLE)

Chaos: sensitive dependence on initial conditions.

Roughly speaking, the MLE of a given orbit characterizes the **mean exponential rate of divergence** of trajectories surrounding it.

Consider an orbit in the  $2N$ -dimensional phase space with **initial condition  $\mathbf{x}(0)$**  and **an initial deviation vector (small perturbation) from it  $\mathbf{v}(0)$** .

Then the mean exponential rate of divergence is:

$$\text{MLE} = \lambda_1 = \lim_{t \rightarrow \infty} \Lambda(t) = \lim_{t \rightarrow \infty} \frac{1}{t} \ln \frac{\|\mathbf{v}(t)\|}{\|\mathbf{v}(0)\|}$$

$\lambda_1 = 0 \rightarrow$  Regular motion ( $\Lambda \propto t^{-1}$ )

$\lambda_1 > 0 \rightarrow$  Chaotic motion

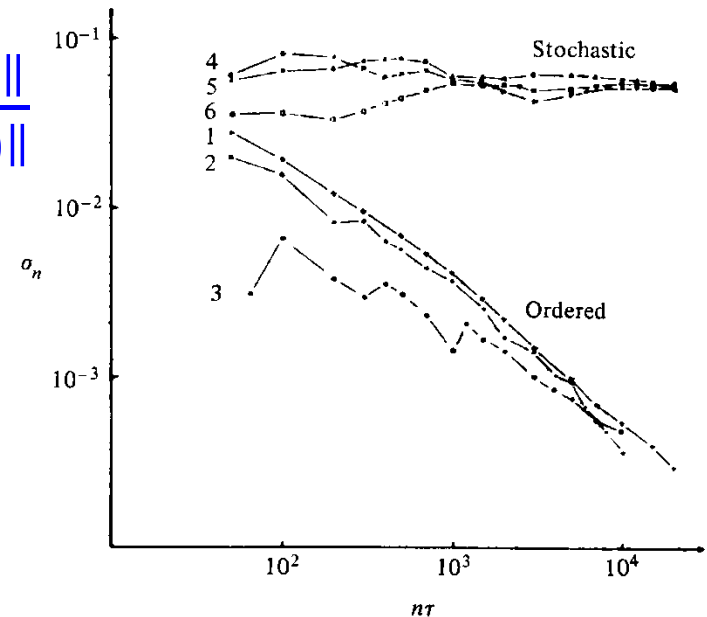
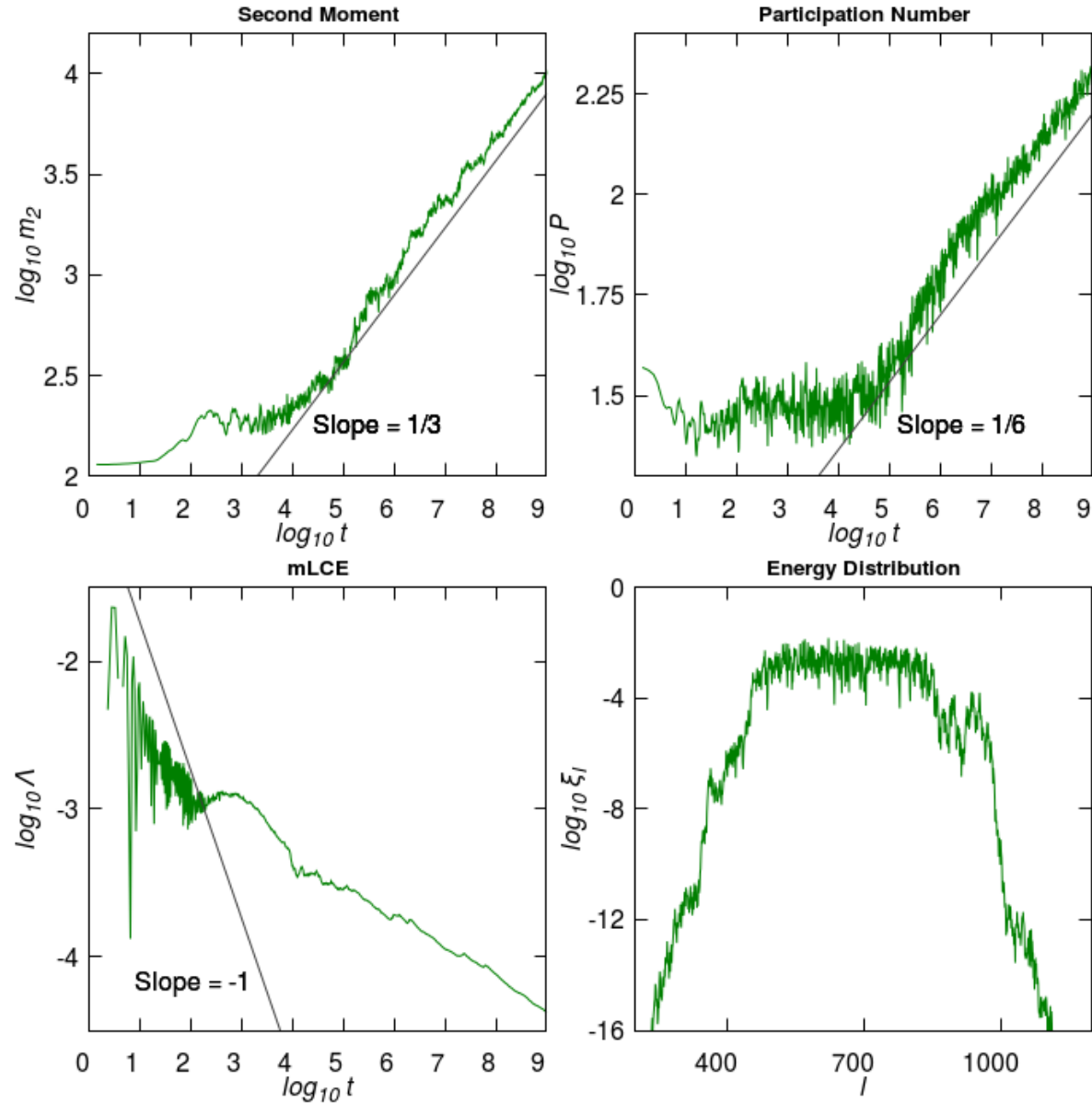


Figure 5.7. Behavior of  $\sigma_n$  at the intermediate energy  $E = 0.125$  for initial points taken in the ordered (curves 1–3) or stochastic (curves 4–6) regions (after Benettin *et al.*, 1976).

# A weak chaos case

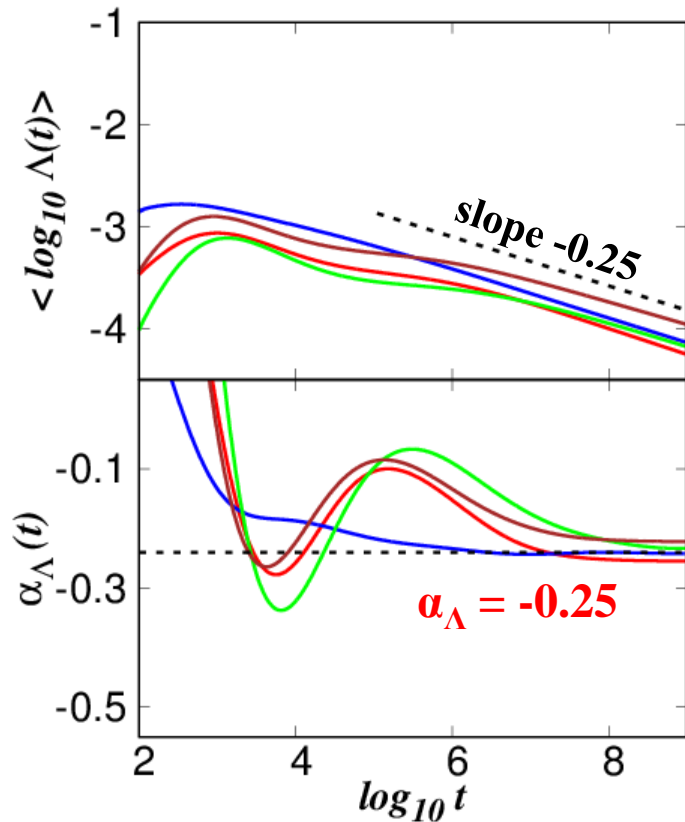
Block excitation  
 $L=37$  sites,  
 $H=0.37$ ,  $W=3$ .

One disorder  
realization

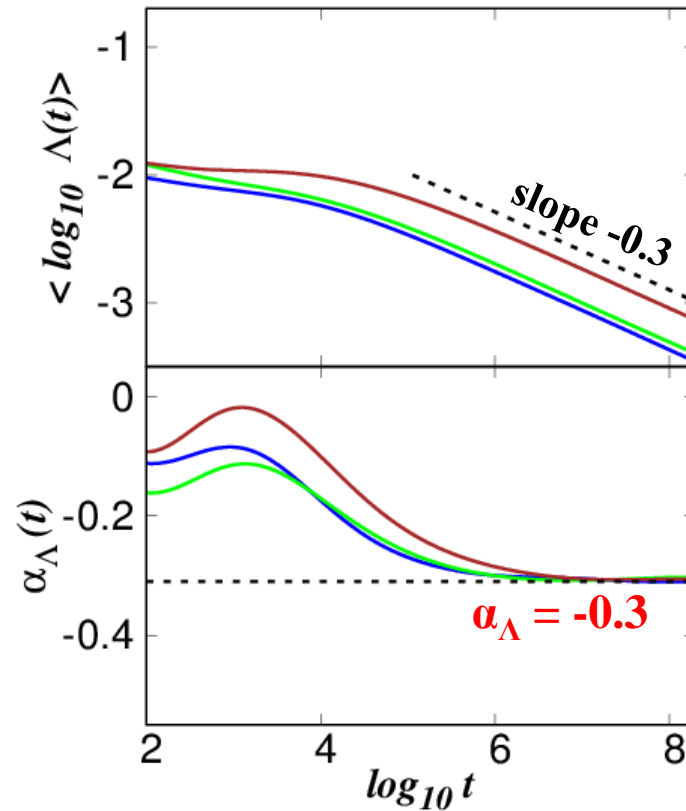


# Time evolution of the MLE: $\Lambda \propto t^{\alpha_\Lambda}$

**Weak  
chaos**



**Strong  
chaos**



Average over 100 realizations [Senyange et al., PRE (2018)]

**Block excitation (L=37 sites) H=0.37, W=3**

**Single site excitation H=0.4, W=4**

**Block excitation (L=21 sites) H=0.21, W=4**

**Block excitation (L=13 sites) H=0.26, W=5**

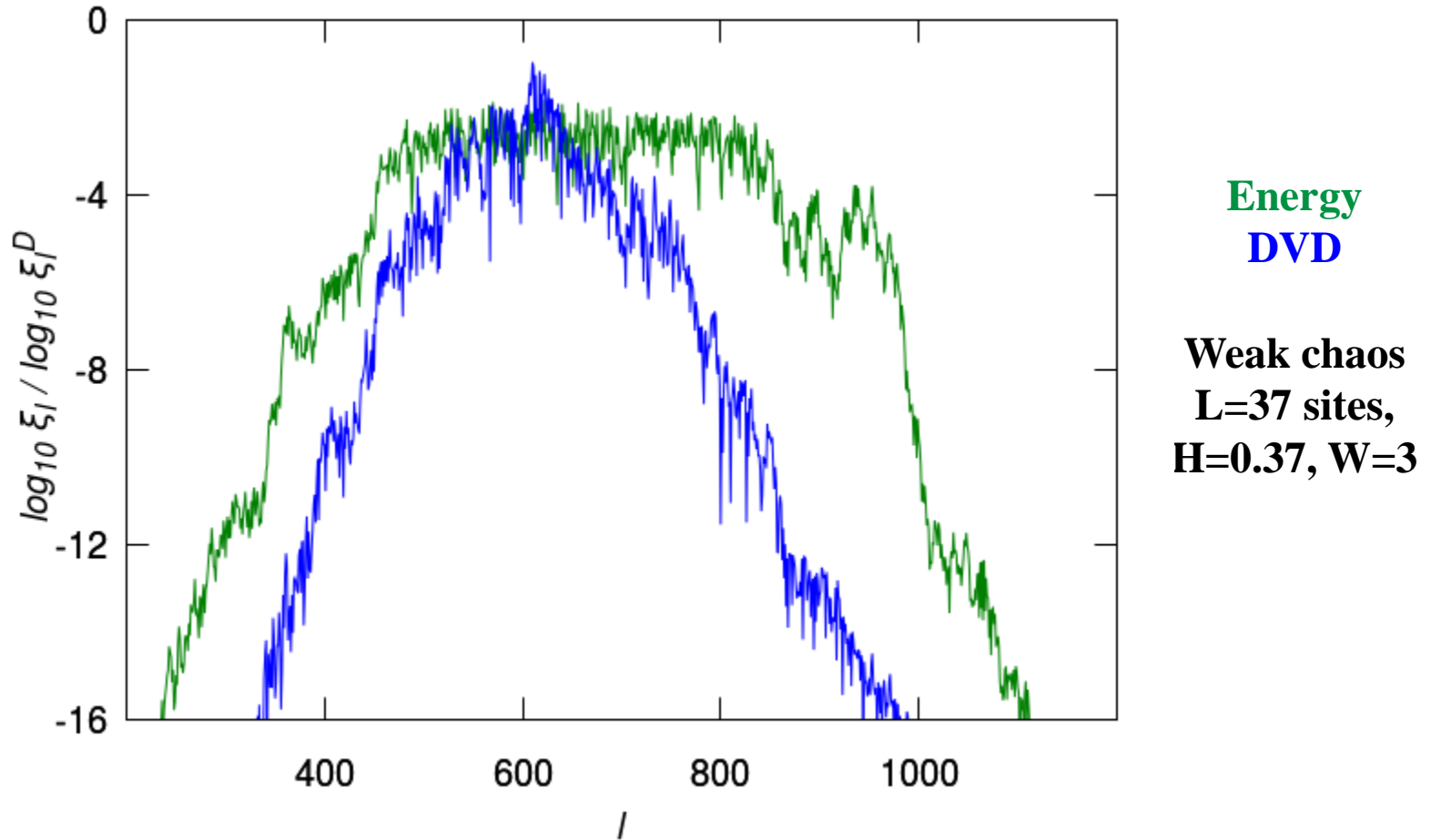
**Block excitation (L=83 sites) H=0.83, W=2**

**Block excitation (L=37 sites) H=0.37, W=3**

**Block excitation (L=83 sites) H=0.83, W=3**

The weak chaos case was also studied in S. et al., PRL (2013)

# Deviation Vector Distributions (DVDs)



**Deviation vector:**

$$\mathbf{v}(t) = (\delta u_1(t), \delta u_2(t), \dots, \delta u_N(t), \delta p_1(t), \delta p_2(t), \dots, \delta p_N(t))$$

$$\mathbf{DVD}: \xi_l^D = \frac{\delta u_l^2 + \delta p_l^2}{\sum_l (\delta u_l^2 + \delta p_l^2)}$$

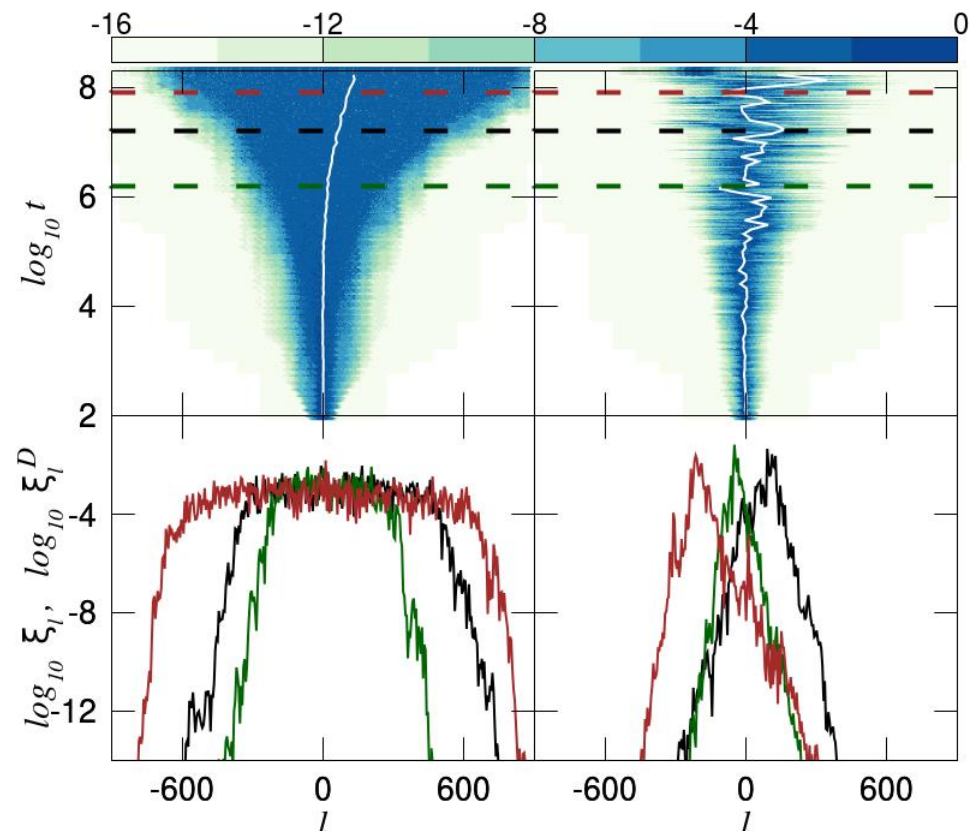
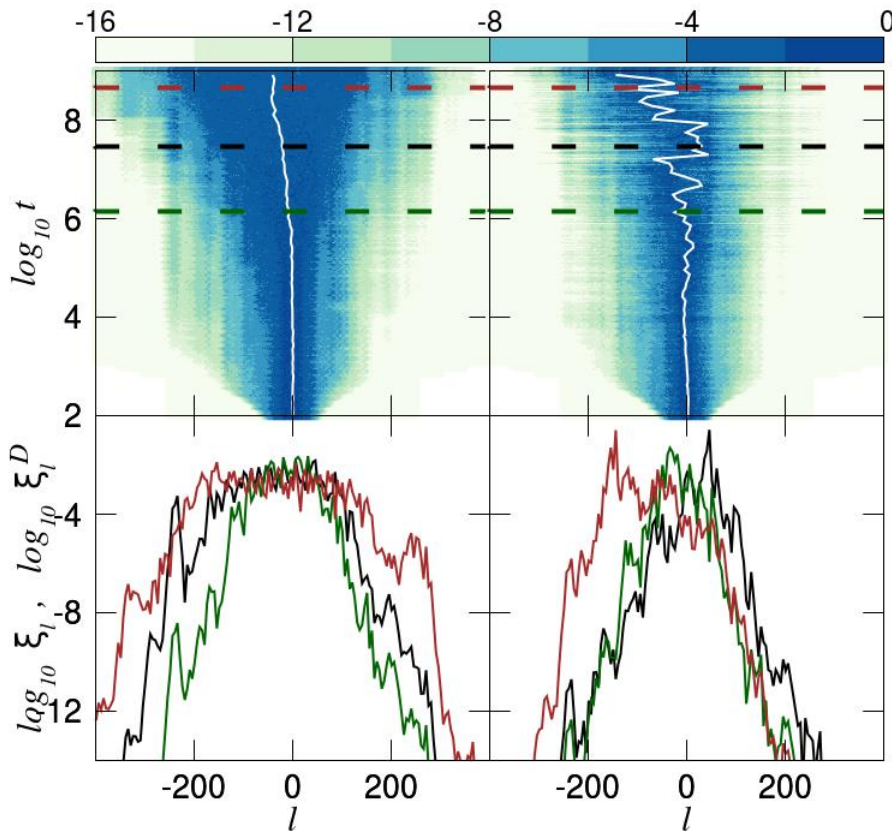
# DVDs: Weak and Strong Chaos

Weak chaos

Strong chaos

Energy DVD

Energy DVD



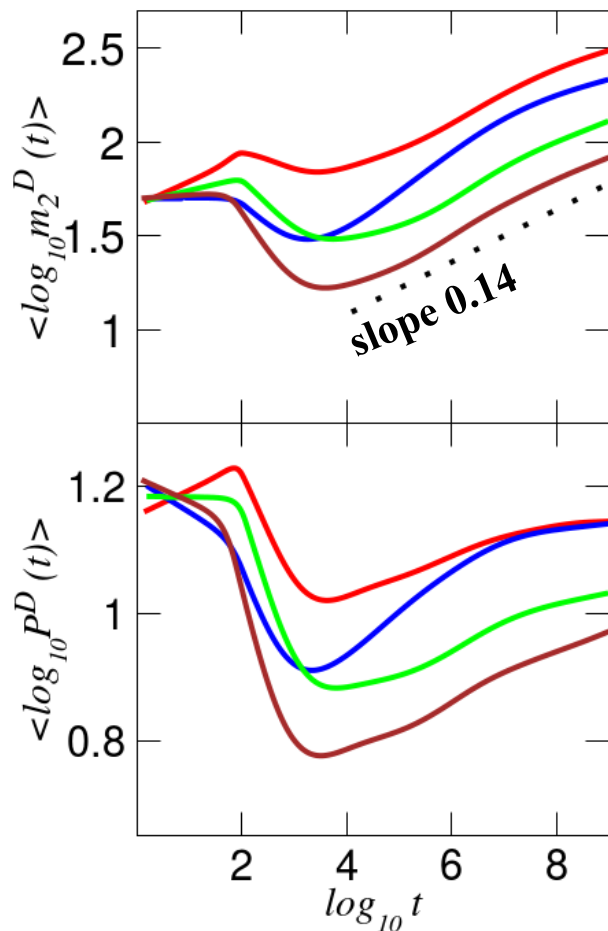
$W=3, L=37, H=0.37$

$W=3, L=83, H=8.3$

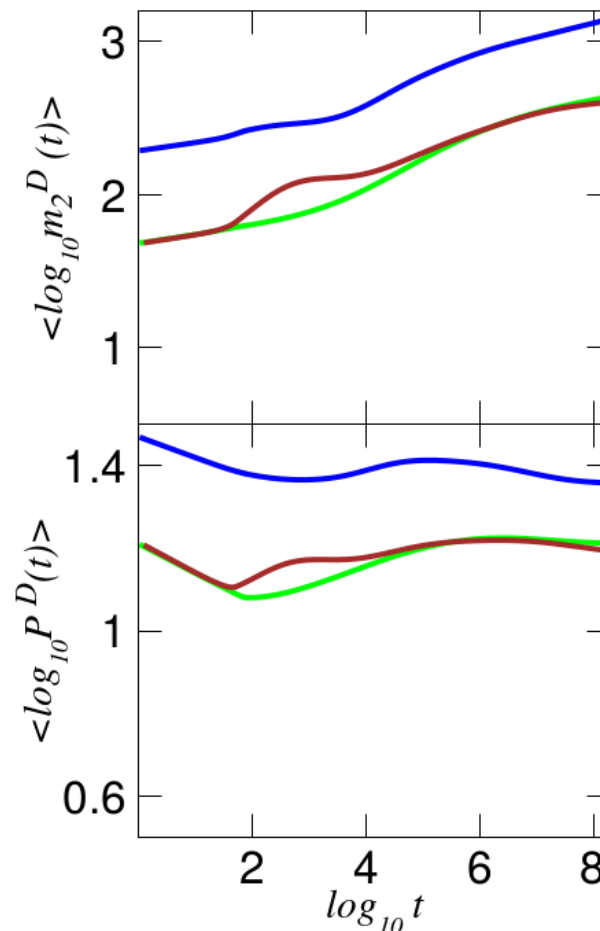
**Chaotic hot spots meander through the system, supporting the homogeneity of chaos inside the wave packet.**

# Characteristics of DVDs

## Weak chaos



## Strong chaos

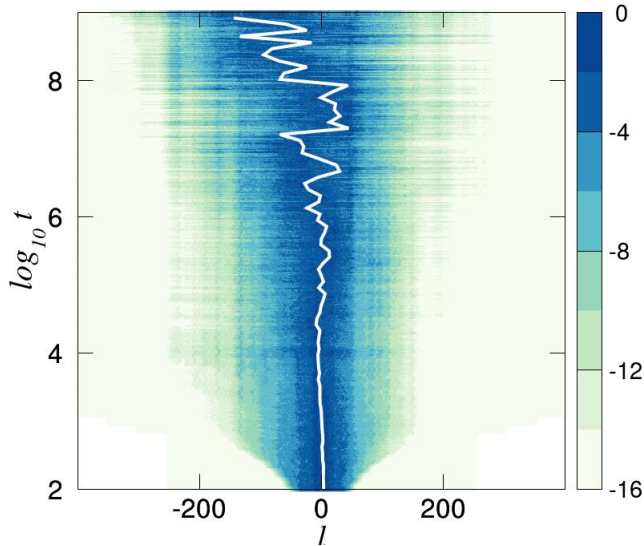


**The DVD remains very concentrated: a rather small number of sites are highly chaotic at each time.**

# Characteristics of DVDs

Weak chaos

$L=37, H=0.37, W=3$

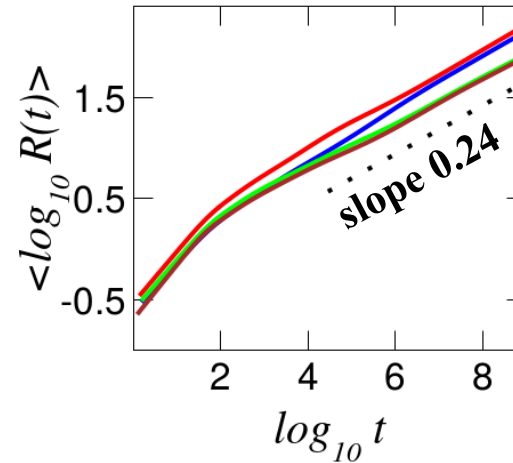


Range of the lattice  
visited by the DVD

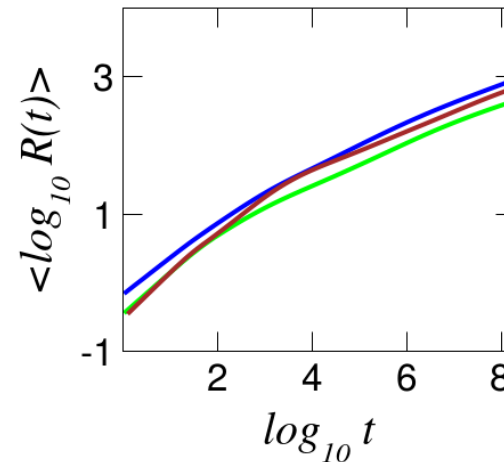
$$R(t) = \max_{[0,t]} \{ \bar{l}_w(t) \} - \min_{[0,t]} \{ \bar{l}_w(t) \}$$

$$\bar{l}_w = \sum_{l=1}^N l \xi_l^D$$

**The DVD exhibits oscillations, whose amplitudes increase in time (larger amplitudes for strong chaos) in order to visit all regions inside the spreading wave packet.**



Weak  
chaos



Strong  
chaos

# Frequency Map Analysis (FMA)

Compute the **fundamental frequencies**,  $f_1$  and  $f_2$ , of an observable related to the evolution of an orbit in **two successive time windows** of the same length, and check **whether or not these frequencies change in time** [Laskar, Icarus (1990) – Laskar et al., Physica D (1992) – Laskar, Physica D (1993) – Robutel & Laskar, Icarus (2000)].

**Regular motion:** The computed frequencies do not vary in time

**Chaotic motion:** The computed frequencies vary in time

For every lattice site  $l$  we compute the fundamental frequencies  $f_{1l}$  and  $f_{2l}$  for time windows of length  $T = 6 \cdot 10^5$  time units and evaluate the **relative change of these two frequencies**:

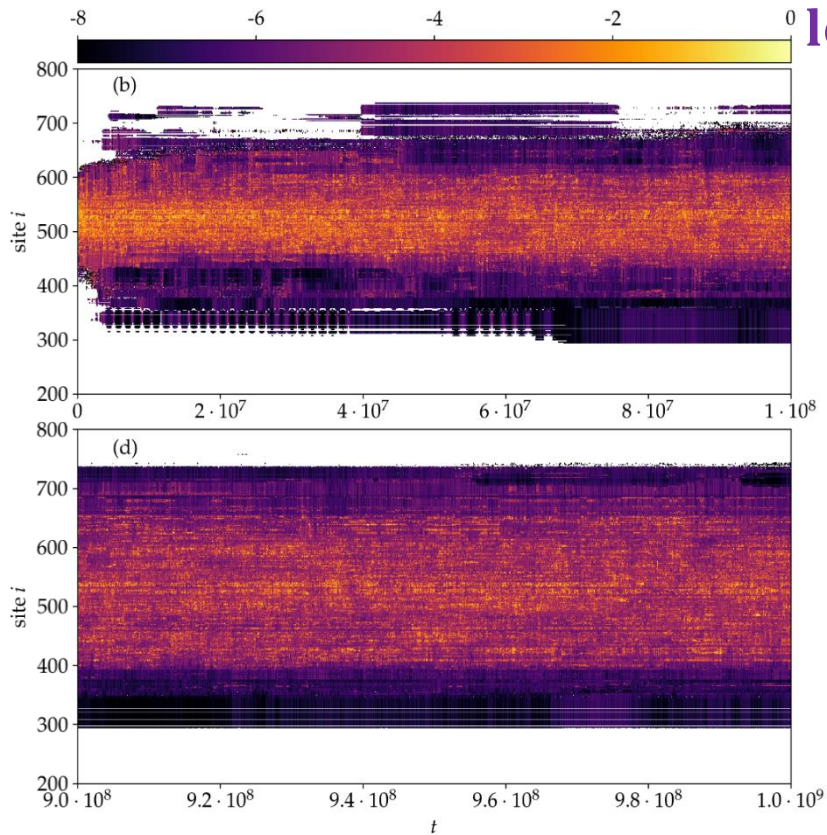
$$D_l = \left| \frac{f_{2l} - f_{1l}}{f_{1l}} \right|$$

**Regular motion:** small  $D_l$  values

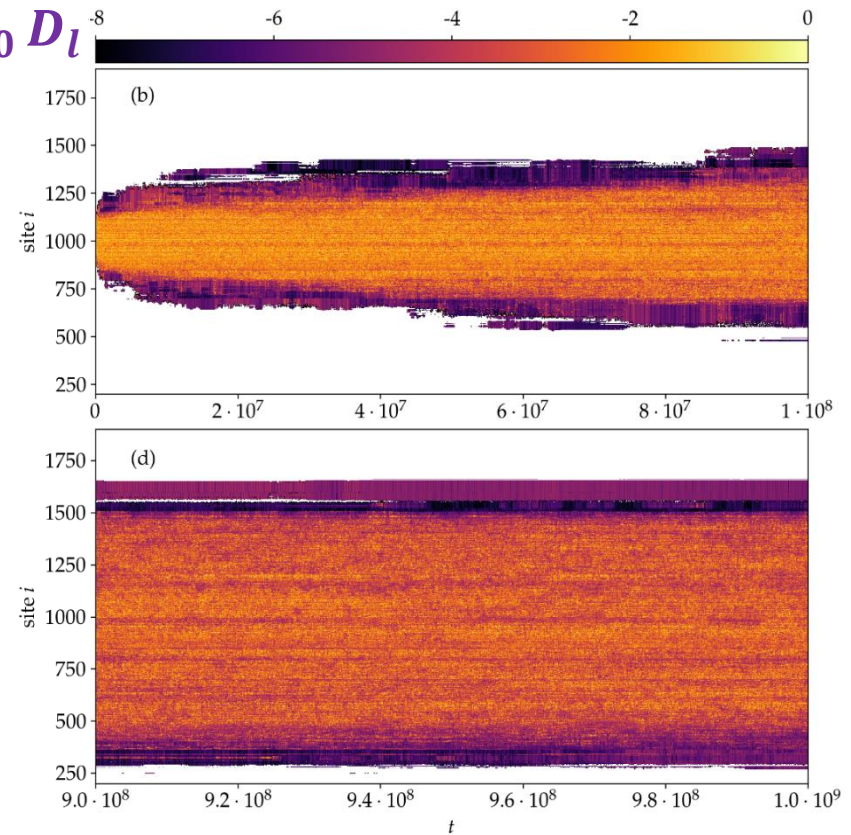
**Chaotic motion:** large  $D_l$  values

# FMA: Weak and Strong Chaos

Weak chaos  
 $L=1, H=0.4, W=4, N=999$



Strong chaos  
 $L=21, H=4.2, W=4, N=3499$



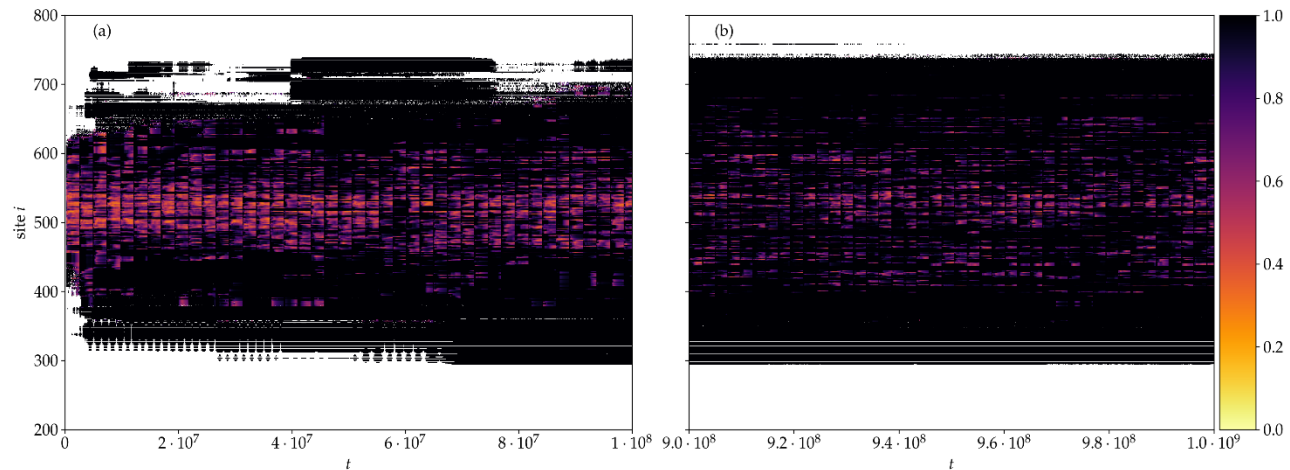
**Chaotic behavior appears at the central regions** of the wave packet, where the energy density is relatively large. The chaotic component of the wave packet **is more extended in the strong chaos case** [S. et al., IJBC (2022)]

# Frequency Locking (FL)

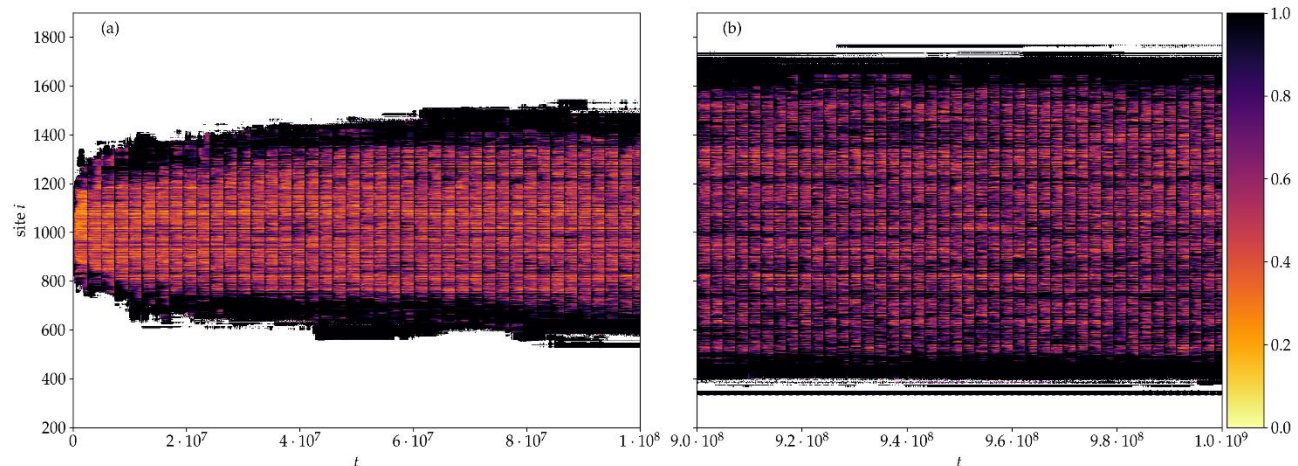
Frequency bins of width  $10^{-4}$ . For each lattice site and a duration of  $t = 2.4 \cdot 10^7$  we compute the fundamental frequencies in 200 time windows and register the related bins.

**$FL_i$ : the fraction of the most visited bin ( $0 \leq FL_i \leq 1$ ). Measures the degree of practical frequency constancy (denoting nonchaotic behavior) of each oscillator.**

Weak chaos



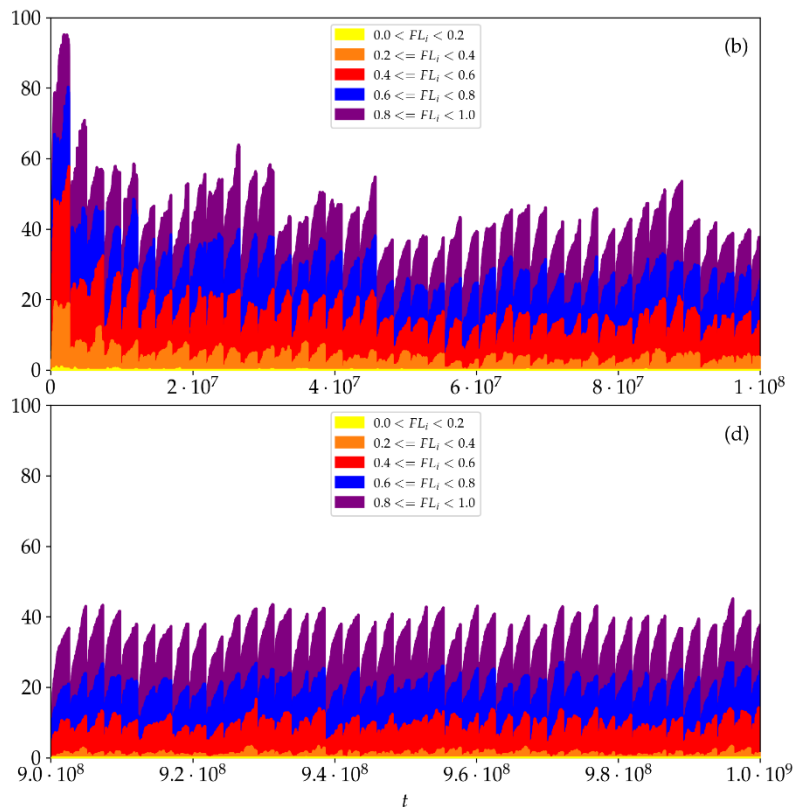
Strong chaos



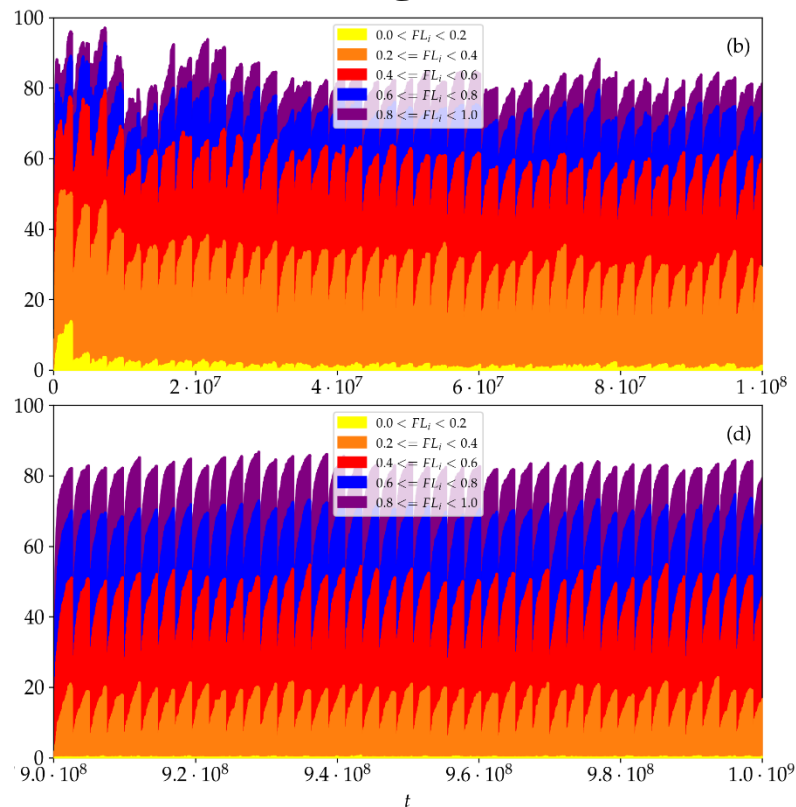
# Frequency Locking (FL)

Accumulated percentages  $P_{FL}$  of sites with values in a particular  $FL$  range

Weak chaos



Strong chaos



The fraction of **sites behaving chaotically** is much larger in the strong chaos regime.

The percentage of **strongly chaotic sites (having  $FL_i < 0.4$ )** is about 5 times larger for strong chaos.

For **both spreading regimes, the fraction of highly chaotic oscillators ( $FL_i < 0.4$ ) decreases in time**, although the percentage of chaotic sites remains practically constant.

# The Generalized Alignment Index (GALI)

In the case of an  $N$  degree of freedom Hamiltonian system or a  $2N$  symplectic map we follow the evolution of

$k$  deviation vectors with  $2 \leq k \leq 2N$ ,

and define [S. et al., Physica D, (2007)] the **Generalized Alignment Index (GALI)** of order  $k$  :

$$GALI_k(t) = \|\hat{v}_1(t) \wedge \hat{v}_2(t) \wedge \dots \wedge \hat{v}_k(t)\|$$

where

$$\hat{v}_1(t) = \frac{v_1(t)}{\|v_1(t)\|}$$

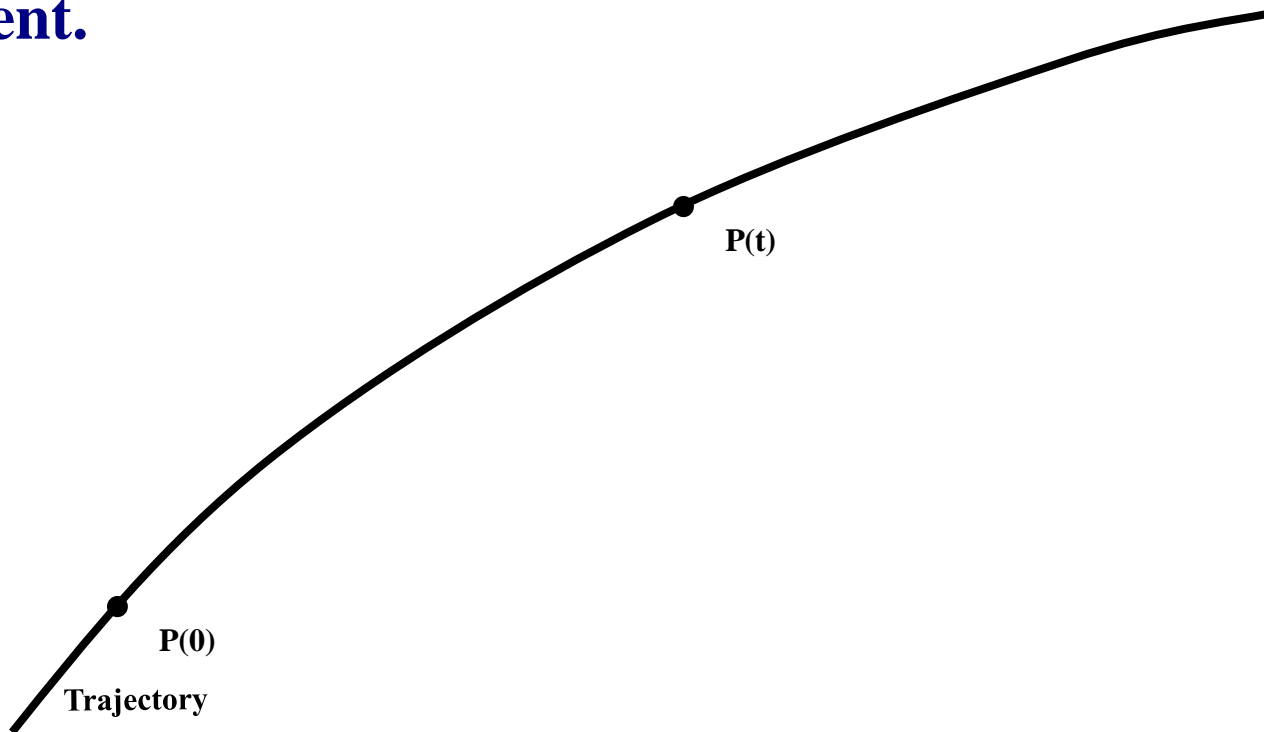
$GALI_k$  is defined as **the volume of the parallelepiped** formed by the  $k$  normalized deviation vectors

# **Behavior of deviation vectors for chaotic motion**

**For chaotic orbits two initially different deviation vectors tend to coincide with the direction defined by the maximum Lyapunov exponent.**

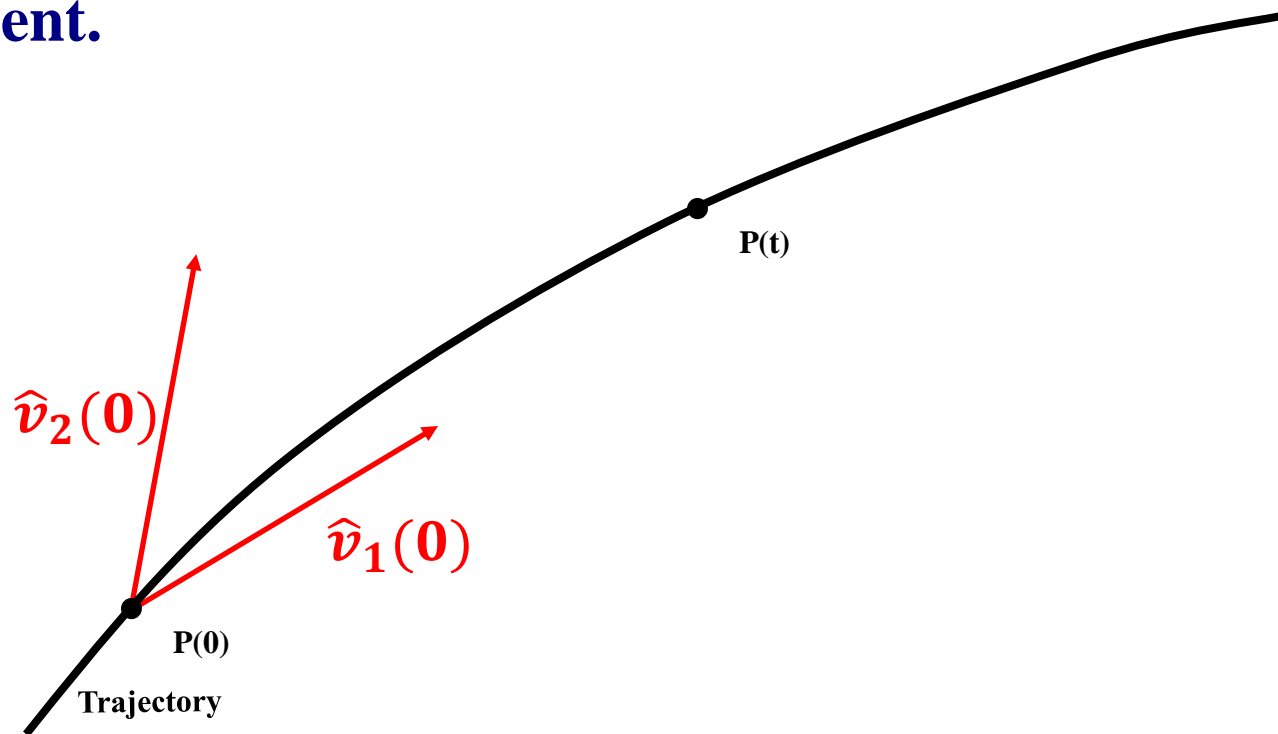
# Behavior of deviation vectors for chaotic motion

For chaotic orbits two initially different deviation vectors tend to coincide with the direction defined by the maximum Lyapunov exponent.



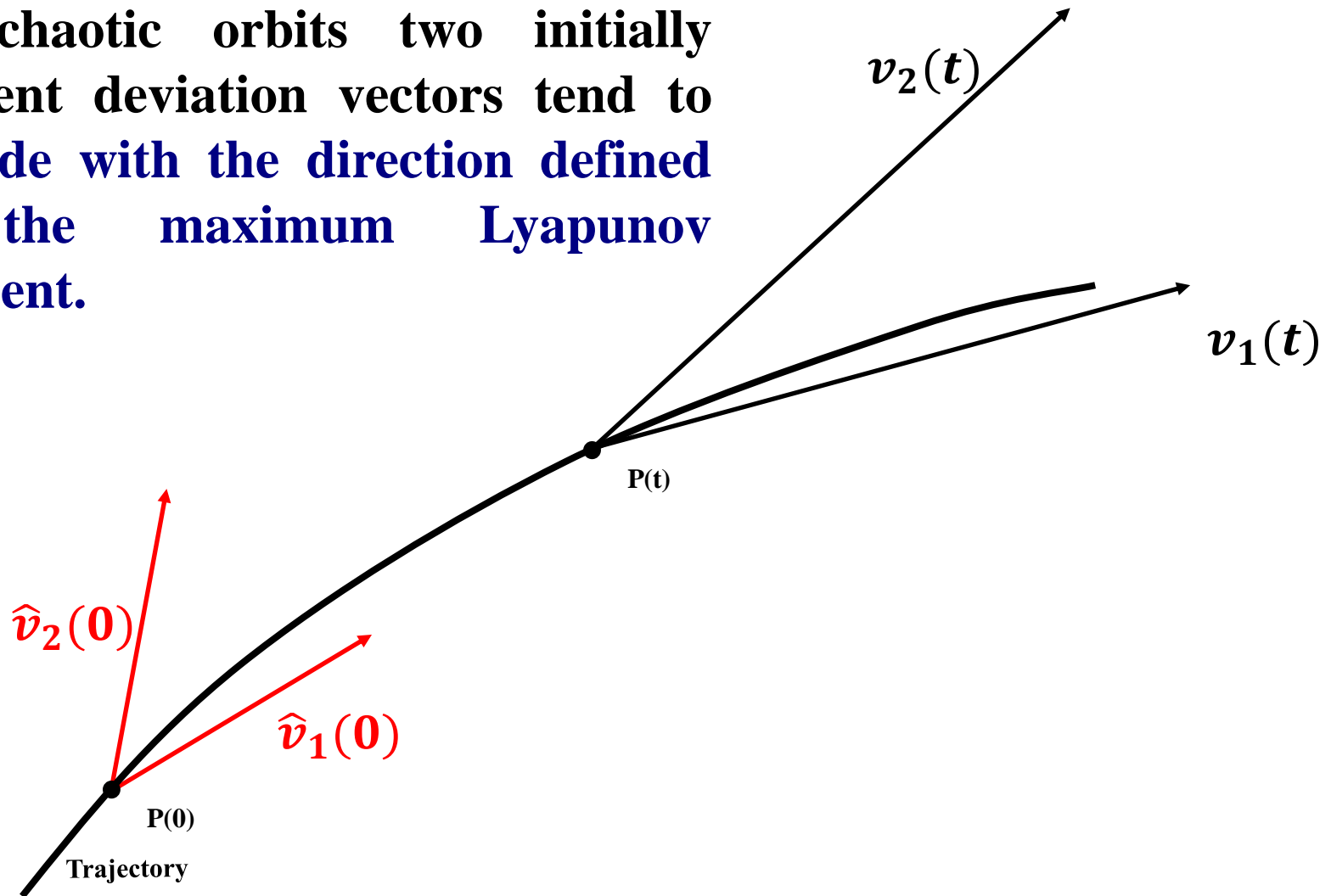
# Behavior of deviation vectors for chaotic motion

For chaotic orbits two initially different deviation vectors tend to coincide with the direction defined by the maximum Lyapunov exponent.



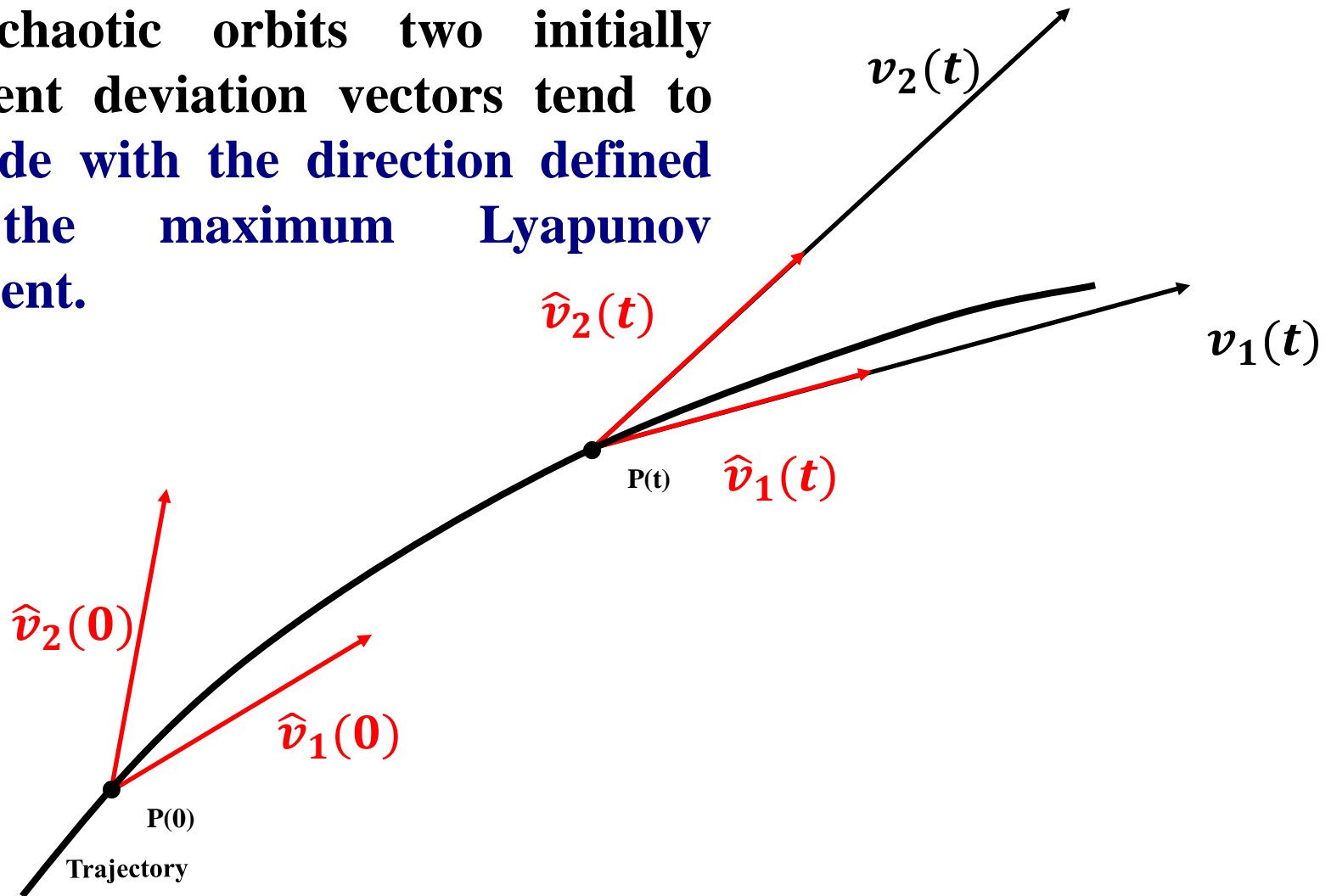
# Behavior of deviation vectors for chaotic motion

For chaotic orbits two initially different deviation vectors tend to coincide with the direction defined by the maximum Lyapunov exponent.



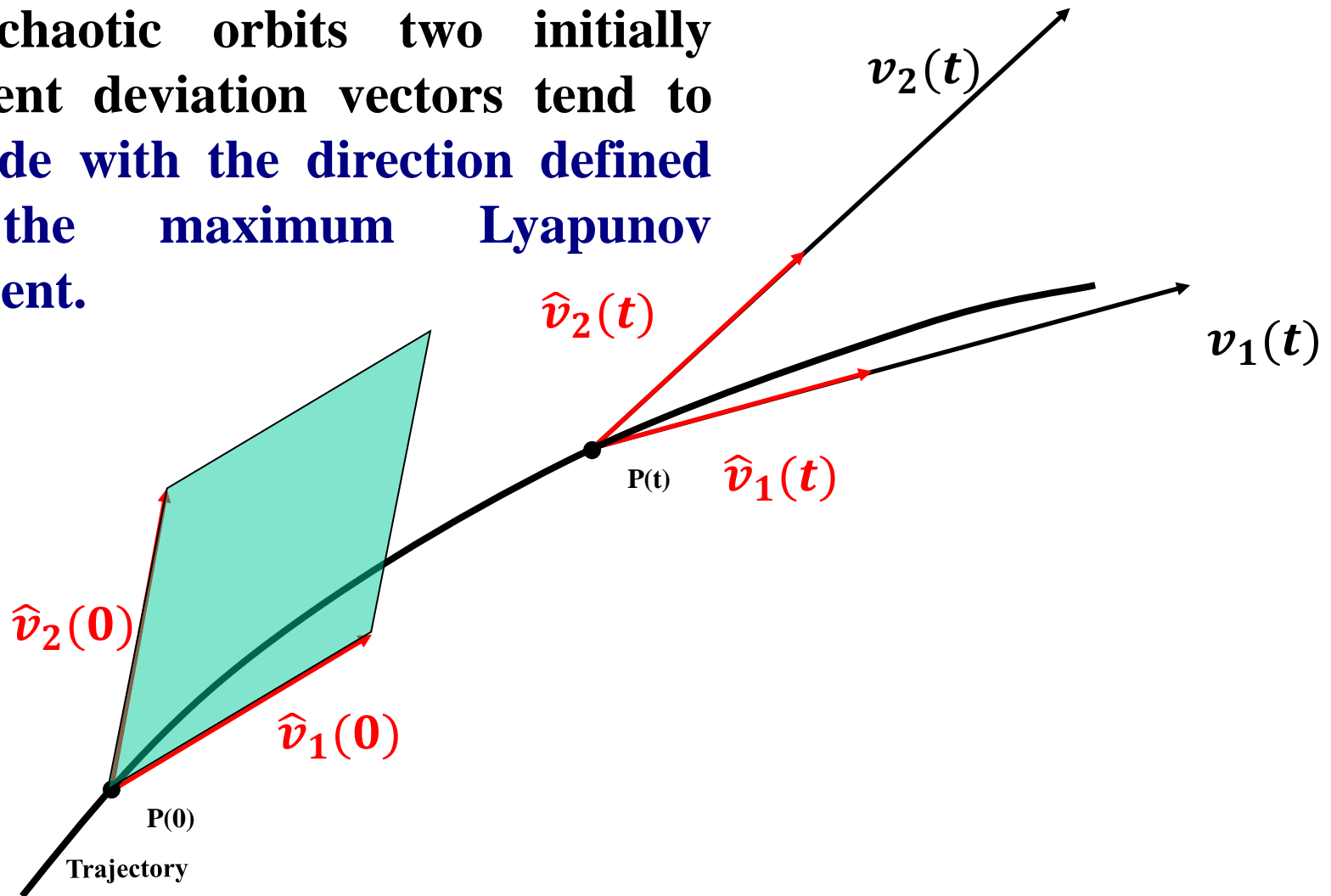
# Behavior of deviation vectors for chaotic motion

For chaotic orbits two initially different deviation vectors tend to coincide with the direction defined by the maximum Lyapunov exponent.



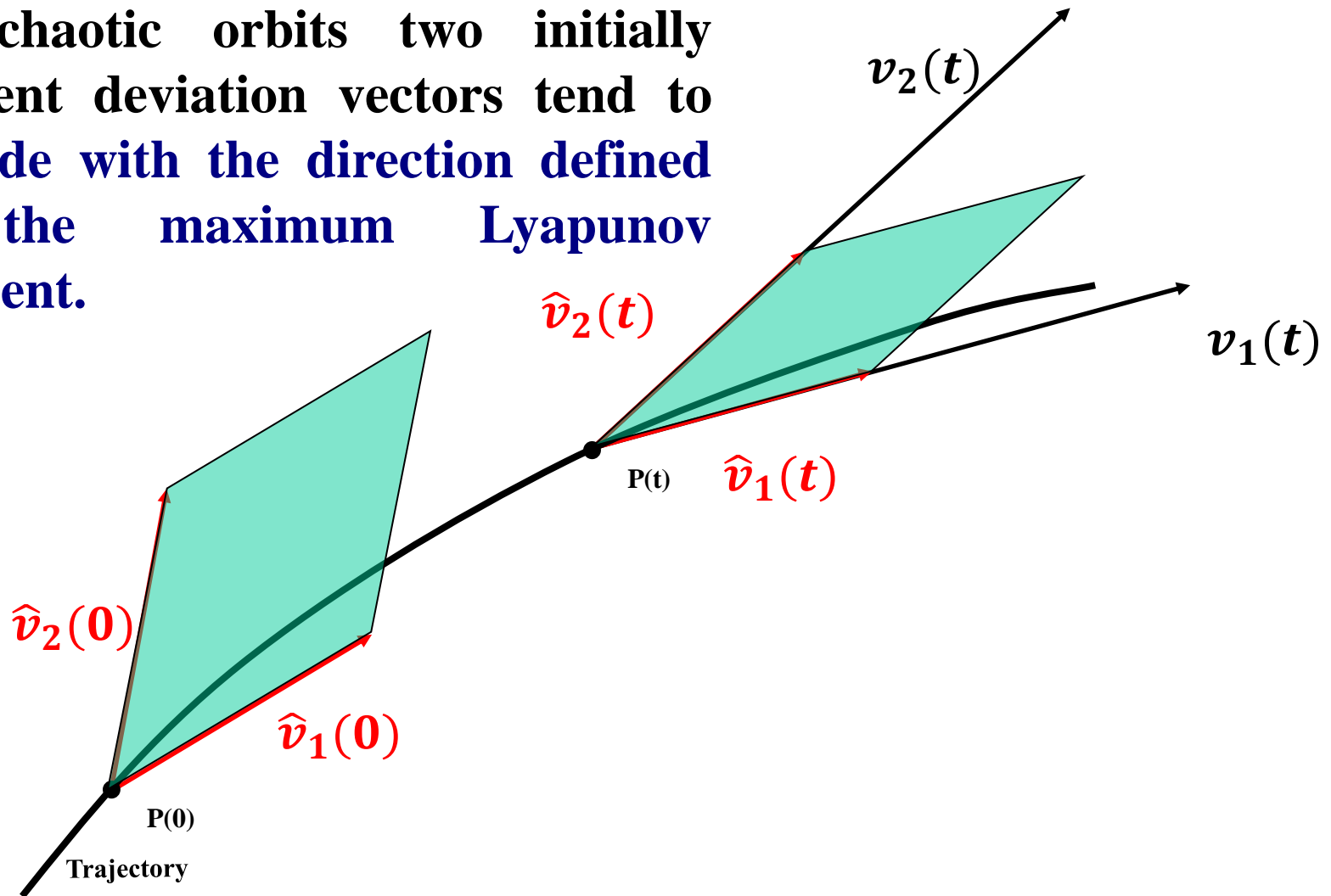
# Behavior of deviation vectors for chaotic motion

For chaotic orbits two initially different deviation vectors tend to coincide with the direction defined by the maximum Lyapunov exponent.



# Behavior of deviation vectors for chaotic motion

For chaotic orbits two initially different deviation vectors tend to coincide with the direction defined by the maximum Lyapunov exponent.

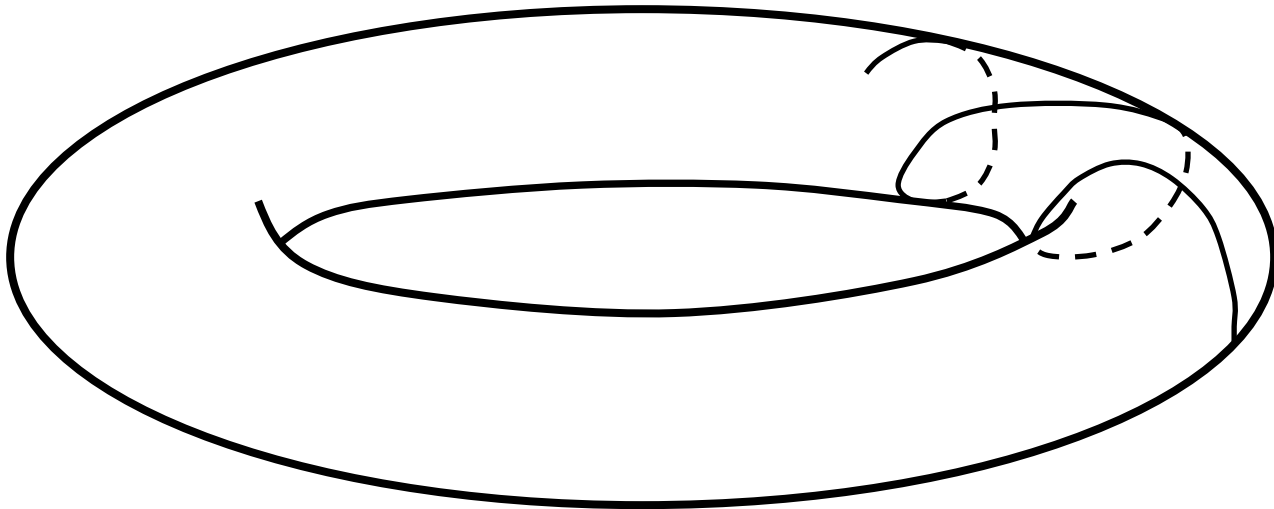


## **Behavior of deviation vectors for regular motion**

**Regular motion occurs on a torus and two different initial deviation vectors become tangent to the torus, generally having different directions.**

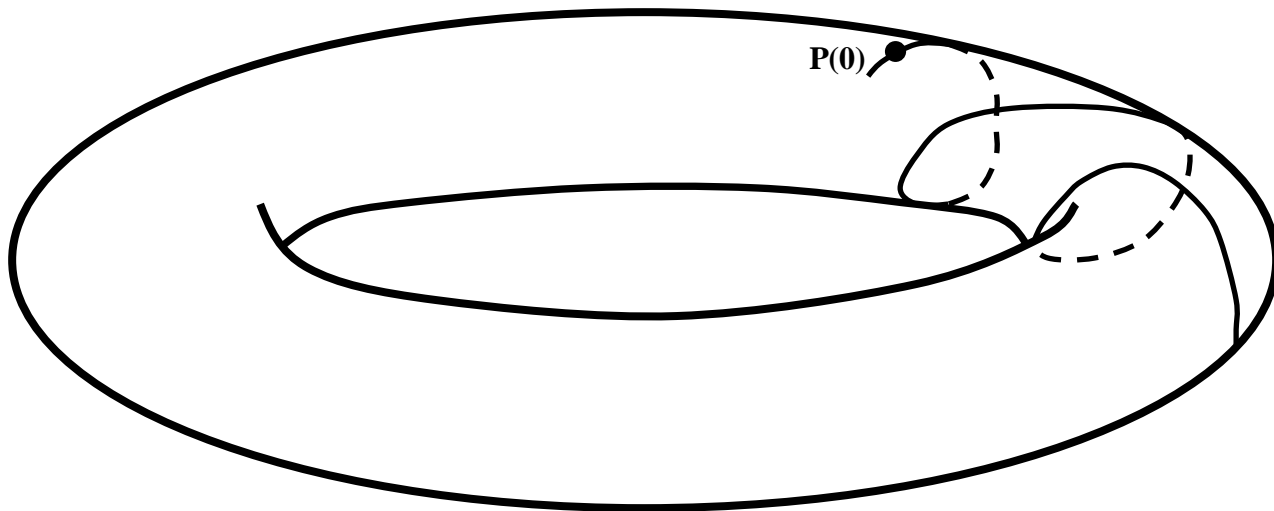
## Behavior of deviation vectors for **regular motion**

Regular motion occurs on a torus and two different initial deviation vectors **become tangent to the torus, generally having different directions.**



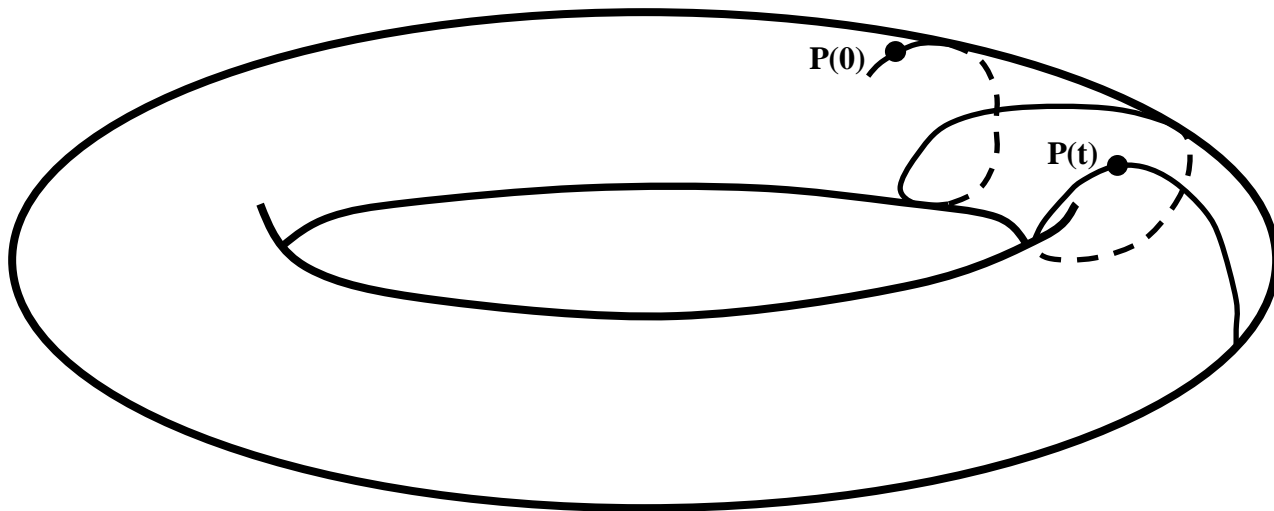
# Behavior of deviation vectors for **regular motion**

Regular motion occurs on a torus and two different initial deviation vectors **become tangent to the torus, generally having different directions.**



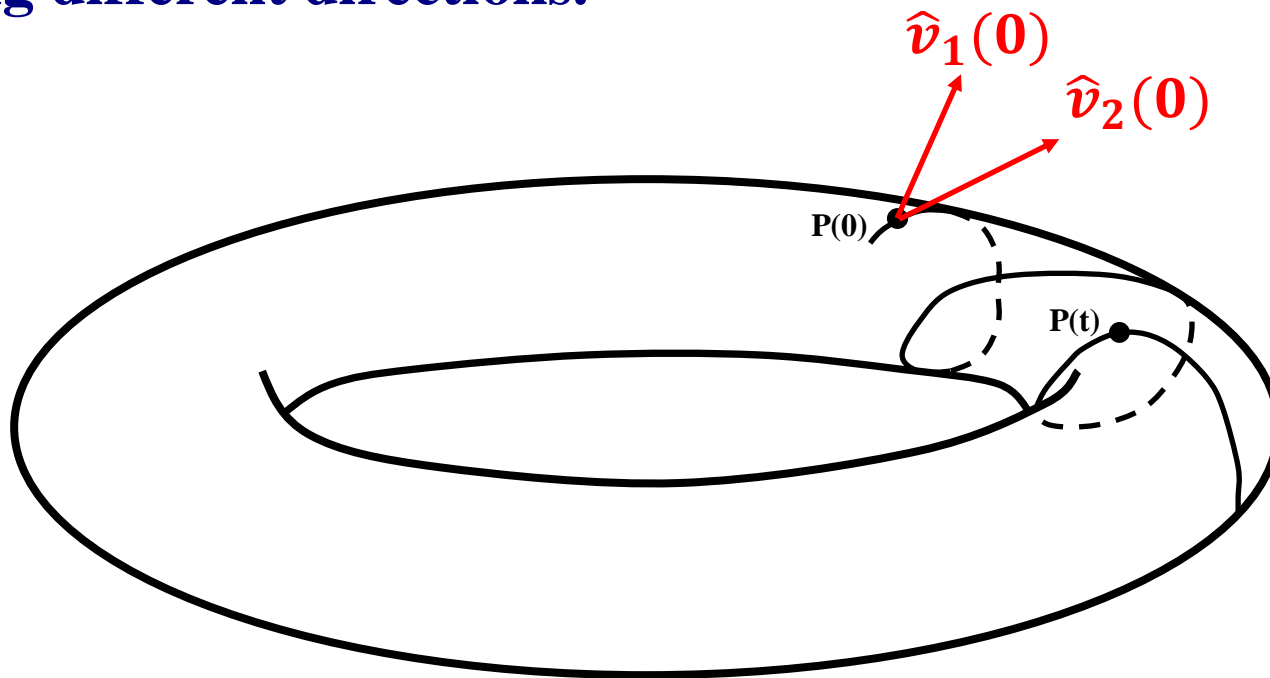
# Behavior of deviation vectors for **regular motion**

Regular motion occurs on a torus and two different initial deviation vectors **become tangent to the torus, generally having different directions.**



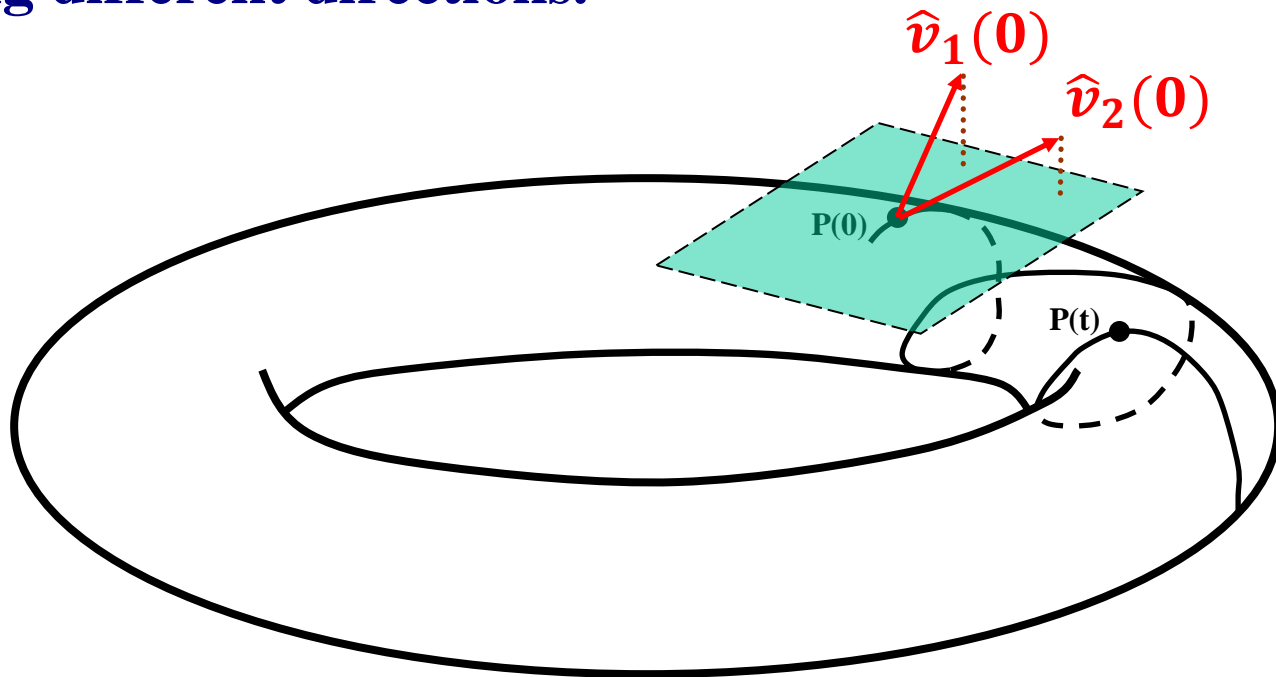
# Behavior of deviation vectors for **regular motion**

Regular motion occurs on a torus and two different initial deviation vectors **become tangent to the torus, generally having different directions.**



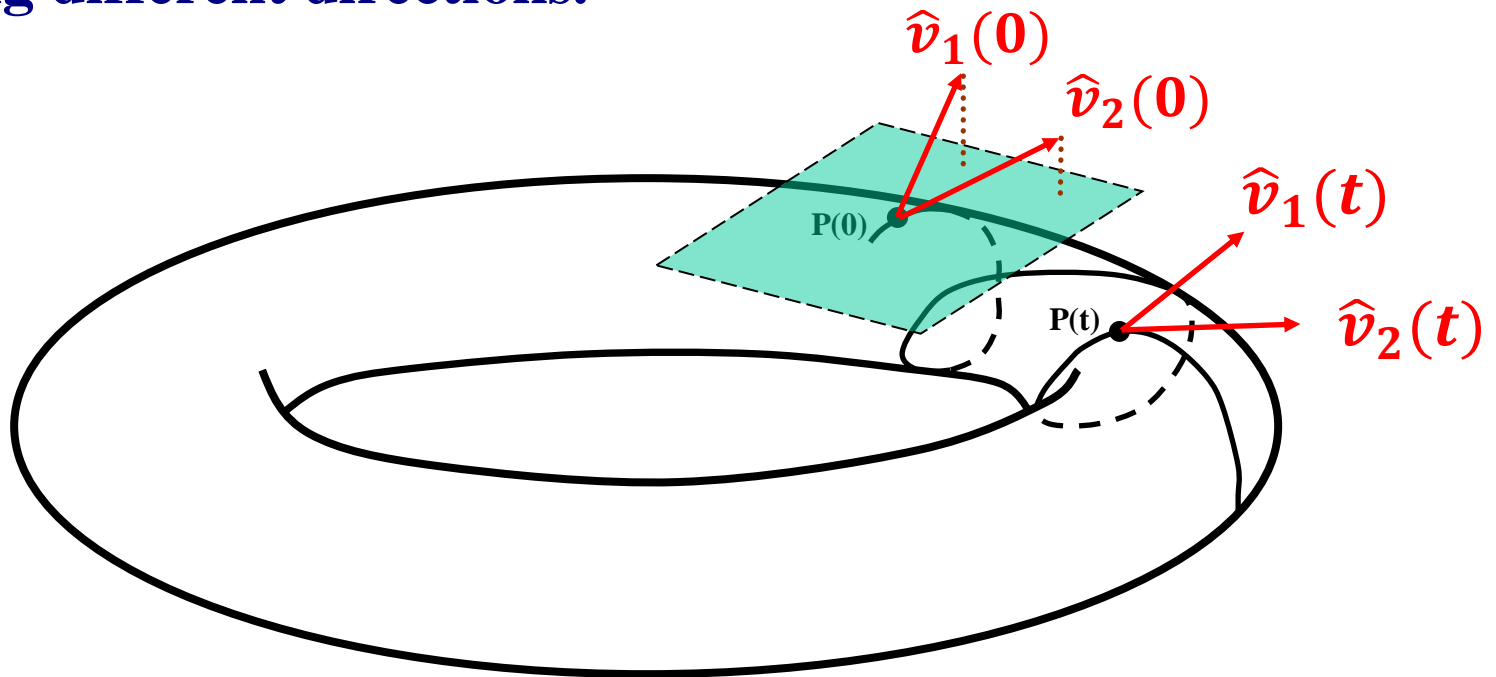
# Behavior of deviation vectors for regular motion

Regular motion occurs on a torus and two different initial deviation vectors become tangent to the torus, generally having different directions.



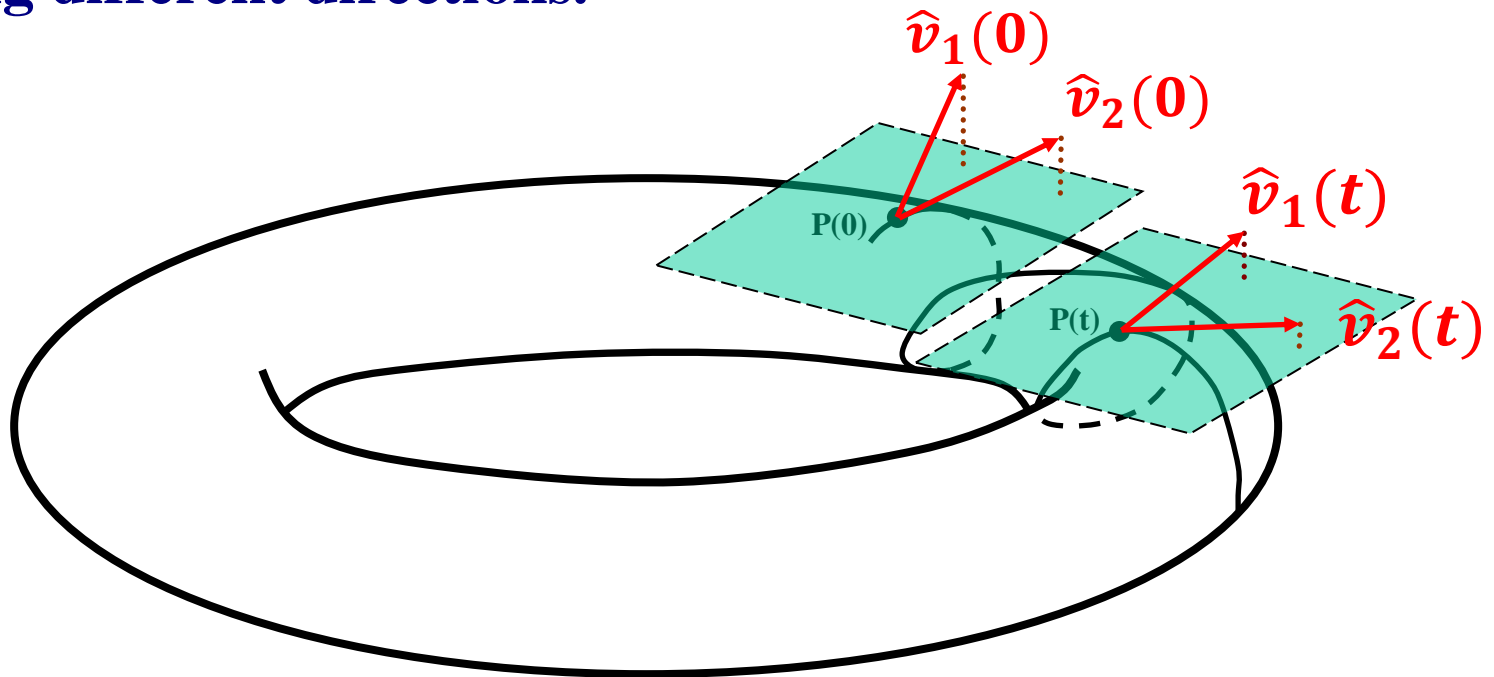
# Behavior of deviation vectors for regular motion

Regular motion occurs on a torus and two different initial deviation vectors become tangent to the torus, generally having different directions.



# Behavior of deviation vectors for regular motion

Regular motion occurs on a torus and two different initial deviation vectors become tangent to the torus, generally having different directions.



# Behavior of the $GALI_k$

**Chaotic motion:**  $GALI_k$  ( $2 \leq k \leq 2N$ ) tends exponentially to zero with exponents which involve the values of the first  $k$  largest Lyapunov exponents  $\lambda_1, \lambda_2, \dots, \lambda_k$ :

$$GALI_k(t) \propto e^{-[(\lambda_1 - \lambda_2) + (\lambda_1 - \lambda_3) + \dots + (\lambda_1 - \lambda_k)]t}$$

**Regular motion:** When the motion occurs on an  $N$ -dimensional torus then the behavior of  $GALI_k$  is given by [S. et al., Eur. Phys. J. Sp. Top. (2008)]:

$$GALI_k(t) \propto \begin{cases} \text{constant} & \text{if } 2 \leq k \leq N \\ \frac{1}{t^{2(k-N)}} & \text{if } N < k \leq 2N \end{cases}$$

Here we only consider  $GALI_2$  ( $k=2$ ) which is equivalent to the **Smaller Alignment Index (SALI)** [S, J. Phys A (2001)].

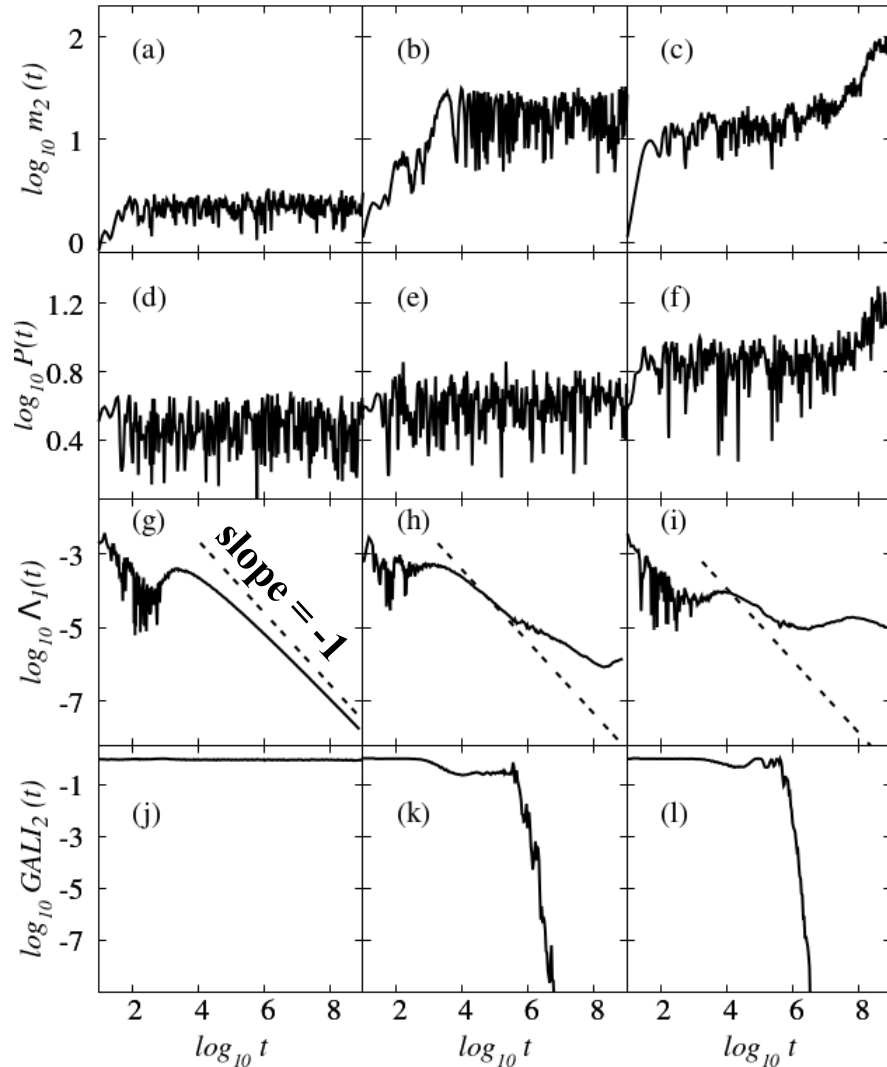
# Regular vs. chaotic (localized or spreading) motion

Different disorder realizations can exhibit different behaviors.

Regular  
motion

Localized  
chaos

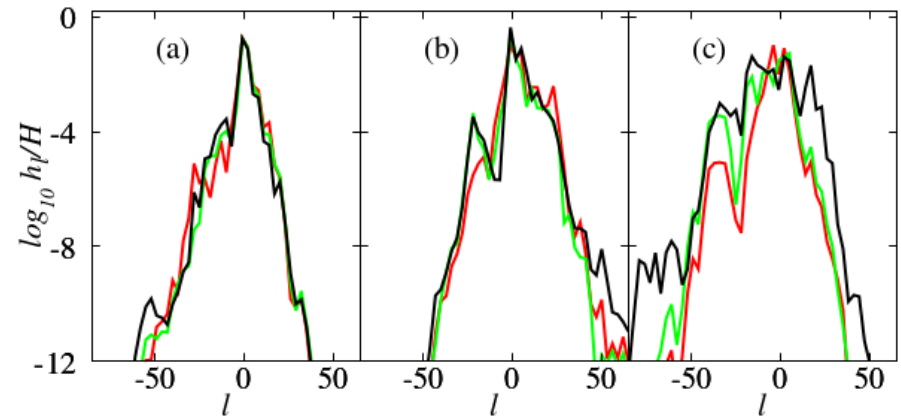
Spreading  
chaos



Regular  
motion

Localized  
chaos

Spreading  
chaos



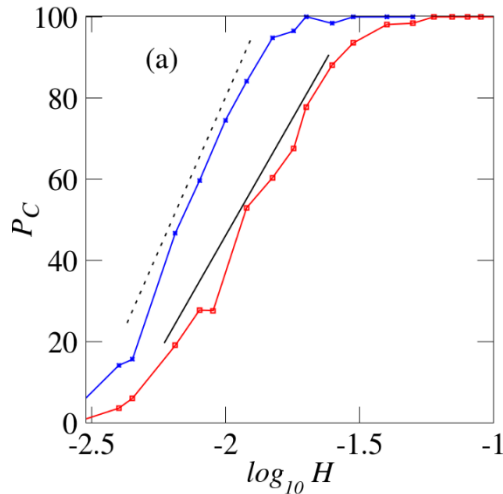
$$t = 10^5, 10^7, 10^9$$

Single site excitations,  $L=1$ , for  
 $W=6$ ,  $H=0.02$  [Senyange & S.,  
Physica D (2022)].

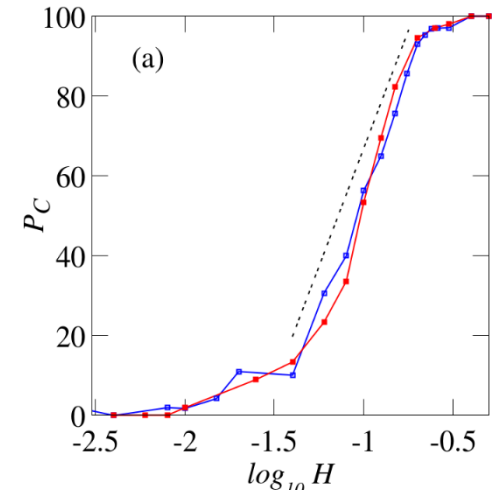
The  $\text{GALI}_2$  can identify chaos  
much more clearly than the MLE.

# Decreasing nonlinearity

## Single site excitations



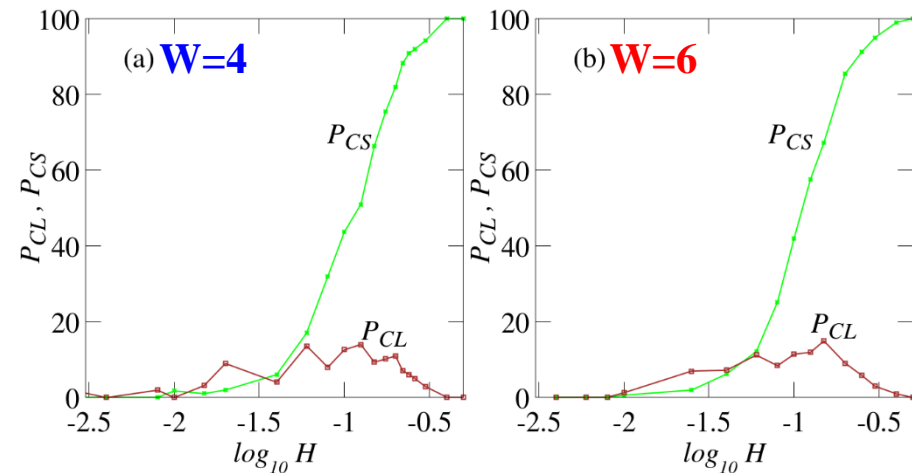
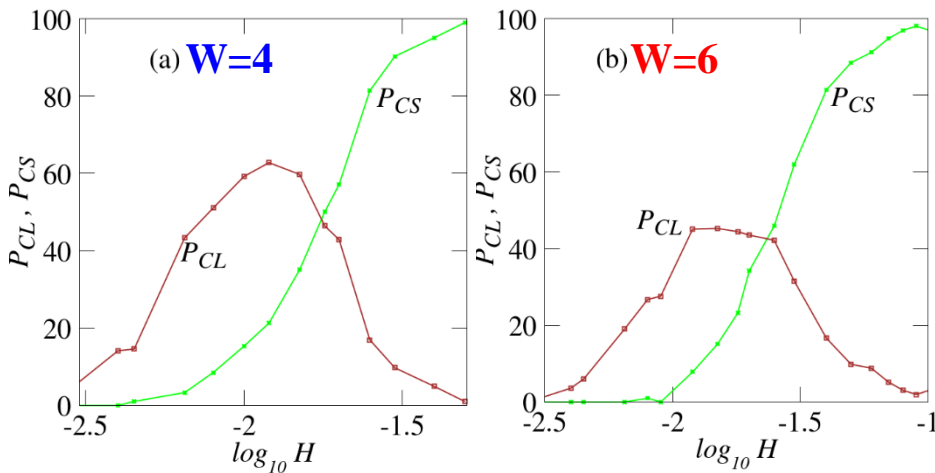
## Single mode excitations



$P_C$ : % of chaotic orbits

$W=4$ ,  $W=6$

$P_{CL}$ : % of localized chaos  $P_{CS}$ : % of spreading chaos



**Energy thresholds** for transition to regular motion and to spreading chaos are lower for single site excitations which permit mode interactions [Senyange & S., Physica D (2022)].

# Summary

We investigated in depth the spatiotemporal chaotic behavior of the DKG multidimensional Hamiltonian system.

- **Identification of 2 different dynamical spreading regimes: weak and strong chaos**
- **The MLE reveals the decrease of the system's chaoticity in time**  
Weak chaos:  $\Lambda \propto t^{-0.25}$  - Strong chaos:  $\Lambda \propto t^{-0.30}$
- **The DVDs provide information about the propagation of chaos**  
Wandering of localized **chaotic hot spots** in the lattice's excited part homogenize chaos.
- **FMA computations uncover the characteristics of chaos evolution**  
Chaotic behavior appears at the central regions of the wave packet, being more pronounced in the strong chaos case.
- **The GALI method allows the detailed study of the system's behavior when it approaches its linear limit**  
Clear identification of chaos.  
Efficient distinction between **localized and spreading chaos**.  
Identification of **energy thresholds** leading to global chaotic spreading and to the total absence of chaos.

# Main references

- **S. (2001) J. Phys. A, 34, 10029**
- **S., Bountis, Antonopoulos (2007) Physica D, 231, 30**
- **S., Bountis, Antonopoulos (2008) Eur. Phys. J. Sp. Top., 165, 5**
- **Flach, Krimer, S. (2009) PRL, 102, 024101**
- **S., Flach (2010) PRE, 82, 016208**
- **Laptyeva, Bodyfelt, Krimer, S., Flach (2010) EPL, 91, 30001**
- **Bodyfelt, Laptyeva, S., Krimer, Flach (2011) PRE, 84, 016205**
- **S., Gkolas, Flach (2013) PRL, 111, 064101**
- **Senyange, Many Manda, S. (2018) PRE, 98, 052229**
- **Senyange, S. (2022) Physica D, 432, 133154**
- **S., Gerlach, Flach (2022) Int. J. Bifurc. Chaos, 32, 2250074**